Caudal Granular Insular Cortex and the Maintenance of Allodynic behavior in the Rat

Serhiy Chumachenko

Department of Psychology and Neuroscience

University of Colorado at Boulder

October 31, 2011

Thesis Adviser: Daniel S. Barth, Ph. D.

Honors Committee: Matthew C. Keller, Ph. D., Kevin R. Jones, Ph. D.

Table of Contents

Abstract

While mechanical allodynia, a disorder characterized by perception of generally acceptable stimuli as painful, is relatively pervasive, little is known about its mechanism of onset and maintenance, and few treatments exist for it. Recent studies of allodynia have begun to focus on a limited number of cortical areas as a potential mediator, however, a newly elucidated caudal granular region of the insular cortex (CGIC), has not yet been investigated. In this study, inactivation of CGIC in rats and its effect on allodynia is studied both behaviorally and electrophysiologically. A spine-CGIC-primary-somatosensory-cortex-spine signaling loop is then proposed as a possible mechanism of allodynia maintenance.

Caudal Granular Insular Cortex and the Maintenance of Allodynic behavior in the Rat

Chronic pain, characterized by pain that persists beyond the normal tissue healing period, is a disorder present in millions of individuals worldwide (Elliott, Smith, Penny, Smith, & Chambers, 1999). Previous investigations of chronic pain and allodynia (a disorder where typically innocuous tactile stimuli are perceived as painful) have focused on the role of the peripheral nervous system (PNS) or the spinal cord (Campbell & Meyer, 2006) as a possible cause and site of modulation of these disorders. Recently, studies have also begun to give attention to cortical modulation as a key player in pain disorders. For example, the insular cortex has been linked to chronic pain (Becerra et al., 2006). However, the extent, generalization, mechanism or even the exact localization of cortical pain modulation is not well known, and is under ongoing investigation.

Conceptually, the effects of pain can be divided into two different types, "sensory-discriminative" and "affective-motivational" (Melzack & Casey, 1968; Treede, Kenshalo, Gracely, & Jones, 1999). The former refers to the direct effect of pain; its severity, location, and somatosensory feeling. The latter is much more abstract, and refers to the emotional and psychological effect of pain, such as stress or avoidance, and is accompanied by the appropriate physiological responses such as blood pressure. While sensory-discriminative pain is associated with "higher" function, with cortical modulation known to be carried out by the primary somatosensory cortex (SI), lateral thalamus, and other regions (Peyron, Laurent, & Garcia-Larrea, 2000), similar modulation of sensory-affective pain has not been as well or concretely-described. However, considering how affective-motivational effects of pain are also often associated with "higher" function, a cortical focus in the field of pain has recently developed (Ohara, Vit, & Jasmin, 2005).

Early functional magnetic resonance imaging (fMRI) and positron emission tomography (PET) studies have been carried out to elucidate cortical modulation of pain. They showed that, despite its heavy involvement in many somatosensory functions, SI activation did not correlate as consistently as activation of secondary somatosensory (SII) or insular cortices in response to painful stimuli, where intensity of stimuli above the pain threshold failed to correlate with SI activation (Peyron, Laurent, & Garcia-Larrea, 2000; Derbyshire et al., 1997). Indeed, a relatively low percentage of cells in SI have been found to respond to nociceptive stimuli (Lamour, Willer, & Guilbaud, 1982). As such, other cortical areas were investigated for a link to chronic pain. The prefrontal cortex was found to modulate pain, but at a primarily acute time frame (Lorenz, Minoshima, & Casey, 2003). The anterior cingulate cortex (ACC) was also investigated, and a link was found between chronic pain and activation of this cortical region (Davis et al., 2002). However, altering or reducing ACC function has been shown to only temporarily reduce chronic pain (Li et al., 2010). Therefore, SII and the insular cortices remained as areas with the strongest links to chronic pain (Peyron, Laurent, & Garcia-Larrea, 2000; Peyron et al., 1998; Ostrowsky et al., 2002). However, considering how SII and the insular cortex are often impossible to discriminate in human imaging studies (Brooks, Zambreanu, Godinez, Craig, & Tracey, 2005), the actual role of SII in pain modulation, rather than the insular cortex alone modulating chronic pain, is questionable.

In the investigation of the role of the insular cortex in chronic pain, the rostral agranular region of the insular cortex (RAIC) was an early target region. RAIC was shown to respond or modulate hyperalgesia (Jasmin, Rabkin, Granato, Boudah, & Ohara, 2003), neuropathic pain (Alvarez, Dieb, Hafidi, Voisin, & Dallel, 2009), and allodynia (Coffeen et al., 2011). RAIC was shown to be connected with the amygdala (Reynolds & Zahm, 2005), and involved in anxiety

(Paulus & Stein, 2006), which would suggest a role in the affective-motivational aspect of pain. Despite this strong link of the rostral insula to chronic pain, some laboratories have begun to expand chronic pain investigation to other areas of the insular cortex as well. One of these is the Barth laboratory, in which my honors research has been carried out. A new region of the insula was recently mapped by the Barth laboratory using high-resolution field potential mapping techniques in which it specializes (Benison, Rector, & Barth, 2007). Unlike RAIC, the newly-mapped caudal granular insular cortex (CGIC) has never previously been linked to chronic pain. Despite that, it was shown that CGIC was somatotopically organized (Rodgers, Benison, Klein, & Barth, 2008), suggesting a potential role in the development and maintenance of chronic pain. Therefore, the discovery of CGIC has called for more scrutiny of the insular cortex in its role in chronic pain modulation.

Considering this aforementioned gap in pain literature, the logical next step for my lab after mapping CGIC was to specifically investigate the role of CGIC in pain. My project specifically focused on investigating the effect of CGIC action in the onset and/or modulation of allodynia in rats, and establishing a tentative mechanism of how CGIC accomplishes this. The chronic constriction injury (CCI) model was optimized (Milligan et al., 2006a; Milligan et al., 2006b, Sloane et al., 2009) and used to induce neuropathic pain. The effects of lesioning CGIC on behavioral allodynia measures were investigated. Evoked cortical evoked field potentials and lumbar dorsal horn multi-unit responses were investigated in their timing, localization and ability to be modulated by cortical inactivation.

Methods

All animals were housed and cared for according to guidelines established by the University of Colorado Institutional Animal Care and Use Committee for the humane use of laboratory animals in biological research.

Somatosensory Evoked Potential Mapping

Male Sprague-Dawley rats (300-400g) were anesthetized using the ketamine-xylasine-acepromasine rodent cocktail (KXA, 45, 9 and 1.5 mg drug per kg body weight, respectively) to surgical levels, and were maintained by repeated subsequent KXA injections such that the paw withdrawal reflex was absent, and eye-blink reflex could barely be elicited. A unilateral craniotomy was performed over the right hemisphere, extending from 4mm rostral of bregma to 3mm rostral of lambda and from 1mm medial to the the midsagittal suture to 3mm past the lateral aspect of the temporal bone, exposing a maximal area of the surgically accessible hemisphere. After reflecting the dura, integrity of the cortex was maintained through regular irrigation with Ringer's solution.

Electrophysiological responses in the cortex were recorded using a flat, square multi-electrode array containing 16x16 silver-tipped electrodes (tip diameter, ~100μm; interelectrode spacing, 500μm) covering a 7.5x7.5mm area of the left hemisphere in a single placement (Benison, Rector, & Barth, 2007). The array was positioned onto the cortex so that each electrode was in contact with the animal, and the cortex deformed only slightly, and not enough to alter any electrophysiological function or any aspect of evoked potentials (EPs). All electrodes were referenced to an electrode fastened to the frontal bone of the animal. All signals measured by the array were simultaneously amplified (2000 times), analog filtered (bandpass cutoff, –6 dB at 0.1–3000 Hz; roll-off, 5 dB/octave), and digitized at 10 kHz. EPs were averaged over 64 stimulus presentations.

Electrophysiological responses were elicited via electric stimulation of contralateral forepaw, hindpaw and midtrunk that were shaved and coated with conductive jelly. A bipolar electrode (500μm tips; 1.0mm separation) was used to deliver a biphasic current stimulus from a constant-current source at varying intensities. Auditory click stimuli (0.1ms monophasic pulses) were delivered using a high-frequency piezoelectric speaker placed 15 cm from the contralateral ear.

Insular Excitotoxic Lesions

Animals were anesthetized as previously described using KXA, and were maintained by continuous injection of KXA until sacrifice. Bilaterally, the squamosal and frontal bones were revealed through blunt dissection, and two burr holes were drilled, one burr hole located 4.0mm rostral and 1.0mm dorsal, and another 3.0mm rostral and 0.0mm dorsal to the foramen located on the squamosal bone dorsal to the connection of the zygomatic arch. Subsequently, 0.28μl of NMDA (5% solution) in 0.01 M PBS was injected (twice, at 600 and 300μm depth) by a micro-injector through each burr hole to produce excitotoxic lesions. After the injection, the burr holes were filled with warmed (35°C) paraffin wax (95%) and mineral oil (5%) solution and then covered with dental cement. Postoperative care included subcutaneous administration of 10ml saline, but all analgesics were withheld as to not create confounds with any measures of allodynia. Sham lesions were identically carried out, but NMDA was not pumped through the inserted injector.

Chronic Constriction Injury

Animals were anesthetized using 3% isofluorane in oxygen. The sciatic nerve was exposed using blunt dissection and glass hooks, at a maximal length at the mid-thigh level until branching, and irrigated with Ringer's solution containing the following: 135 NaCl, 3 KCl, 2

MgCl, and 2 CaCl, pH 7.4 (all units are mM, calculated at 37°C). Four chromic gut sutures were loosely tied around the sciatic nerve at even intervals of 1mm; control animals did not receive this treatment. Muscle was sutured back together.

Behavioral Measures – Von Frey Test, Calibrated Toe Pinch

All animals were acclimated to general conditions. On arrival, animals were acclimated to their colony rooms for a minimum of one week prior to testing onset. Each animal was placed into testing conditions for habituation for at least 4 sessions, 20min per session, no more than 2 weeks prior to testing. Each animal was also handled for 5 minutes for 3 consecutive days no more than 2 weeks prior to testing.

A von Frey test was performed as described by Chaplan, Bach, Pogrel, Chung, and Yaksh (1994). A logarithmically calibrated series of up to 10 Semmes–Weinstein monofilaments (von Frey hairs) were applied to the rear portion of the plantar surface of the left and right hindpaws (selected randomly). The selected firmness of the von Frey hairs was gradually increased until hindpaw withdrawal could be reliably (between 3consecutive trials) elicited, with the eliciting firmness being the quantifying measure from which absolute threshold of eliciting stiffness was calculated.

A modified Randall-Stilletto (Luis-Delgado et al., 2006) test was used to measure high-threshold mechanical responses. Four strain-gauge transducers, wired in a full Wheatstone bridge, were connected into a pair of wide forceps. This allowed for quantification of pressure of pinch through the measurement of how much the forceps deformed, where the measurements were transduced with a strain meter. The device was calibrated using known weights used to deform the forceps, and so all stored and observed pressure data was accordingly recorded in grams.

Animals were gently wrapped in a blanket to calm them and somewhat restrain movement. The prepared forceps were then used to compress the hindpaw of the rat parallel to the dorsal-palmar axis, at the center of the foot. Pressure was applied with linearly increasing intensity (which the experimenter was able to monitor while proceeding with the toe pinch) at the rate of 67g/sec, until observable withdrawal occurred.

Spinal Laminar Multi-Unit Recording

A laminectomy was carried out to remove the dorsal half of three vertebrae over the lumbar enlargement, and dura was reflected. Ringer's solution was used as previously described for the cortex to preserve spinal integrity. The sciatic nerve was exposed as for the CCI surgery, and also irrigated with Ringer's solution until stimulation was needed, after which it was dried and immediately irrigated with mineral oil. Large stereotaxic clamps were used to stabilize the spine, and a single large stainless steel surface electrode (tip diameter, 100μm) was used to map the largest contralateral spinal response to direct sciatic stimulation (1.0ms square biphasic pulses, at minimum current sufficient to evoke reliable responses, generally 0.4–0.6mA) via silver hook electrodes (500μm spacing). Once this area was established, a linear 16-electrode array (10μm^2 contacts, 100μm spacing) was entirely inserted there, and at 1mm lateral of midline.

Evoked potentials from electrodes in the spine were simultaneously amplified (1000x), analog filtered (bandpass cutoff –6 dB at 300–3000 Hz; roll-off, 5 dB/octave), and digitized at 10kHz. Single sciatic-evoked response trials (n=64 for all evoked response trial iterations) were taken for 300ms each for multi-unit analysis. Spinal evoked responses were also recorded during surface cortical stimulation (0.4–0.8mA; 1.0ms biphasic pulses) of CGIC or SI (cortex exposed through previously described craniotomy procedure) by a bipolar stainless steel electrode (0.5

mm contact spacing) stimulating the hindpaw region of the target area, established using the previously described EP mapping method. Sciatic and cortical evoked responses were re-measured after CGIC inactivation using muscimol, where 5µl of 9µM muscimol, dissolved in 0.01 M phosphate buffer (PBS, pH 7.0), was injected ~700µm into target area into the area of maximal sciatic response, and the site was immediately covered with a 1.0-mm-diameter piece of filter paper to prevent muscimol spread. Cortical inactivation was verified by testing for EP absence in CGIC.

Analysis and Groups

For cortical EP mapping of CGIC, 6 animals were used. Sensory response smoothing and final mapping was used by taking the root mean squared (RMS) power (where the largest SI somatosensory EPs were clipped at 50% power to make the smaller CGIC and SII responses more apparent) of the somatosensory or auditory evoked field potential, using bicubic spline interpolation of evoked potential amplitudes across the electrode array. This method has been demonstrated in previous work to have a spatial accuracy of ~80µm (Rodgers et al., 2008). All rostro-caudal dimensions reported in mm (±SEM) and assume bregma as the zero point, and all dorsal-ventral measurements assume the midline as the zero point (the most medial point).

For von Frey behavioral testing groups, two experimental pools were used, one receiving insular lesions prior to CCI ligations, and the other pool receiving CCI ligations first. In pool 1, the experimental group (n=11) received insular lesions while the control group (n=11) received sham lesions, and, after 14 days, both groups received CCI ligations. In Pool 2, both the experimental (n=6) and control (n=6) groups both received CCI ligations, and then, after 14 days (enough time for allodynia to develop) (Sloane et al., 2009), the experimental group received insular lesions while the control group received sham lesions. For both groups von Frey testing

was carried out 90 days after CCI ligation, and was started on the day of the first procedure (prior to it). Testing was done weekly, except after CCI ligation, where testing was then done on days 0, 4, 11, and 14 post-ligation, after which time regular weekly schedule resumed. To ascertain functional termination of CGIC function in lesioned animals, as well as to verify that damage did not spread to other somatosensory areas, functional lesion verification was carried out with n=8, and analyzed in the same manner as in the CGIC EP mapping experiment.

Statistical significance in von Frey measures between CGIC lesion and sham groups was computed using two-way, repeated measures ANOVA, with the first factor consisting of lesion status (CGIC or sham lesion) and the second factor consisting of the time after CCI ligation. *Post hoc* comparison were performed using t tests with the Bonferroni's correction setting thresholds for significance at $p \leq 0.0036$ (0.05/14 comparisons).

To test the effect of CCI lesions on mechanical sensitivity, two groups (n=6 each) were used. One group had received insular lesions, while the other did not. For 5 weeks following insular lesions, low-threshold mechanical sensitivity (von Frey) testing was carried out weekly. Following that, high-threshold mechanical sensitivity (toe pinch) testing was carried out once per animal. Turkey's multiple comparisons test was used for *post hoc* analysis.

For spinal electrophysiology, no experimental controls beside inactivation of CGIC or SI with muscimol were utilized. In the control group (n=4), PBS alone was applied to CGIC, while the experimental group (n=4) received muscimol in PBS. The same group sizes were used in the SI inactivation experiment. All trials for a given stimulation parameter and experimental group were superimposed, where each trial was rectified to have a threshold of sum inclusion to be above pre-stimulus baseline, and normalized to the maximum across electrodes and conditions for a given rat.

Results

Functional Mapping of CGIC

Initial CGIC functional anatomic mapping was used to produce detailed RMS maps of evoked potentials (figure 1). Voltage fluctuations created by postsynaptic dendrite potentials were observed as typical positive-negative waves (1A). SI can be clearly seen as a large dorsal response, and two smaller more ventral signals reflect SII and CGIC (labeled ISF). All three areas (SI, SII and ISF as in each subfigure labels) show focal and separate responses to each stimulus (1B, C and D). It can be seen that CGIC is responsive to somatic stimuli (1A, ISF circle), is somatotopically organized considering varied localization of responses between 1B (at b –2.77 ±0.12mm; m –9.13 ±0.10mm, where b and m refer to distance from bregma and midline, respectively), 1C (b –2.20 ±0.11mm; m +9.30 ±0.08mm) and 1D (b –2.85 ±0.10mm; m +9.05 ±0.11 mm) insular responses. CGIC was also found to have a pronounced auditory area (with maximal response at b, –1.71 ±0.08mm; m, +8.90 ±0.11mm). The superimposed ratunculus was derived from previous studies (Benison et al., 2007).

Functional Lesion Verification

Functional effects of insular lesions on responses to mid-trunk (A), auditory (B) and vibrissal (C) stimulations can be clearly seen on evoked potential RMS maps (figure 2). Outer blue circles (~2mm diameter) represent the extent of functional damage observed. When 2A and 2B are compared to 1B and 1E, respectively, it can be seen that, while the more dorsal SI and SII responses remain relatively unchanged in intensity, the insular absences that should be present in the semitransparent blue circles are absent completely.

Behavioral Effect of CGIC Lesion Before and After CCI

No significant difference (figure 3A) was found when comparing baseline allodynic responses (withdrawal thresholds) between CGIC lesion (triangular points) and sham (square points) animals on the day lesion or sham surgery (figure 3A at -14 days post CCI, p=0.59) and thresholds did not change compared to the subsequent measurement day one week later, prior to CCI ligation (figure 3A at -7 days post CCI, p=.74 for lesion group and .45 for sham group). When CCI ligation is administered 14 days after insular lesions, after a universal allodynic response in all animals (figure 3A at 4 and 11 days post CCI), in sham animals, allodynia was observed to persist up to 90 days after CCI. Meanwhile, compared to shams, response threshold of CGIC lesion animals were shown to significantly recover (p values as shown in figure 3A), nearly to baseline. This effect, both of initial allodynia development for both groups, and then subsequent recovery in pain sensitivity in lesion animals only, was also observed contralaterally to CCI ligations through mirror pain as described by Milligan et al. (2006a) (figure 3B), and allodynic onset and recovery was nearly identical and highly correlated (r=0.98 between corresponding pain thresholds) in magnitude between contralateral (figure 3B, white/outlined points) and ipsilateral (figure 3B, background grey points as taken from figure 3A).

When CCI ligation was administered initially, prior to CGIC lesion or sham surgery, the time course of allodynia development is similar to the previously presented case, where r=0.99 and 0.98 between corresponding ipsilateral (A versus C) and contralateral (B versus D) withdrawal thresholds, respectively. Note that allodynia finishes developing after 11 days, and, as such, CGIC lesions 14 days post-CCI are carried out after allodynia is fully present. As shown by the significance markers in figure 3C, when CGIC lesions were performed, after a ~21 “reversal period” (figure 3C, grey area), allodynia is significantly attenuated in lesion animals (triangular points) as compared to sham animals (square points). Mirror pain development and

attenuation via CGIC lesion was observed in these groups as well, and mirror pain magnitude and time frame was almost identical between contralateral (figure 3D, white/outlined points) and ipsilateral (figure 3D, grey points) hindpaws ($p=0.99$).

Overall, the time course of allodynia recovery after day 11 in CGIC lesioned animals was correlated between experiments where lesions were administered before CCI (figure 3, A and B) or after (figure 3 C and D), both ipsilaterally to CCI (figure 3 A versus C, $r=0.96$) and contralaterally (figure 3 B versus D, $r=0.97$). Two-way ANOVA showed a main effect of CGIC versus sham lesion group status ($p<0.0001$), time ($p<0.0001$), and an interaction effect ($p<0.0001$) in both ipsilateral and contralateral comparisons.

As a control, the effects of CGIC lesion alone on high and low-threshold behavioral pain responses were measured (figure 4A). The effects of bilateral CGIC lesion (triangular points) or sham (square points) on allodynia in both left (grey points) and right (white/outlined points) hindpaws were quantified by the von Frey behavioral measure during the observed reversal period in (figure 3, grey area). Two-way ANOVA showed no effect of CGIC versus sham lesion group status ($p>0.05$), time ($p>0.05$), or an interaction effect ($p>0.05$) in either left or right hindpaw comparisons. After the completion of von Frey testing, animals were also tested for high-threshold mechanical sensitivity using a modified Randall-Selitto method (figure 4B). 21 days after CGIC lesion, no significant difference, in either paw ($p>0.05$), was found between CGIC lesion and sham groups. These findings correspond to the already mentioned lack of difference between pre-CCI insular lesion and sham group baselines seen in figure 3 A and B at 14 and 0 days before CCI.

Spinal Laminar Multi-Unit Responses to CGIC Inactivation

The previously seen effect of CGIC inactivation on allodynia prompted a deeper investigation of the possible effect of CGIC on allodynia through descending modulation. As such, spinal laminar multiunit recording was employed.

Direct CGIC stimulation caused a late (starting at 25.2 ±2.1ms post-stimulation, as seen by the large stimulus artifact at the left edge of the time scale bar) burst of multi-unit activity (MUA) in the spinal cord lumbar enlargement layer 4 (dashed box, where laminar location was computed considering the electrode depth and location) (figure 5A). After isolated CGIC application of muscimol, MUA in response to CGIC stimulation was completely eliminated (figure 5B, as seen in the red traces) compared to control activity (blue traces), indicating that stimulation did not spread to other somatosensory cortical areas, which would otherwise also cause activity in the lumbar enlargement.

Because the previous allodynia experiment (figure 3) focused on areas innervated by the sciatic nerve, direct sciatic stimulation was employed in laminar analysis of the area of the lumbar enlargement most responsive to sciatic stimulation. Sciatic stimulation consistently evoked two bursts of MUA in the spinal cord – a shallow, fast burst (figure 5C, labeled A, with almost immediate onset, in multiple layers at a depth of less than 500μm), and a later, deeper burst (figure 5C, labeled B with the dashed box, with onset with around a 43.1 ±1.4ms latency, in layer 4). The latter response greatly resembled the CGIC-evoked MUA (figure 5A, dashed box), and was indeed eliminated by cortical muscimol application (figure 5D, red traces) when compared with control function (blue traces). While deeper sciatic-evoked MUA was significantly reduced by CGIC inactivation (figure 5E, 500-1000μm, $p=0.012$), more shallow, early sciatic-evoked MUA was left relatively unchanged (figure 5E, 0-400μm, $p=0.82$). Some

attenuation of early ventral sciatic-evoked MUA could be seen in figure 5D (arrow), but this effect did not have significance (p=0.08).

Considering the heavy involvement of SI in somatosensation, its common activity as a cortical relay for much somatosensory information, and some precedent linking it to chronic pain, the possibility of CGIC acting through SI in descending spinal signaling was investigated. Spinal responses to CGIC and sciatic stimulation were observed (figure 6A, C). After inactivation of SI using muscimol, CGIC-evoked MUA in the spinal cord was completely eliminated (figure 6B, new red traces) in layers 4-6 (figure 6F, "CGIC" bars, p=0.0008), and sciatic-evoked MUA was also attenuated (figure 6D, new red traces) in the ventral lamina (figure 6F, "Sciatic" bars, p=0.0002). In the dorsal layers, neither SCIC-evoked (p=0.12) nor sciatic-evoked (p=0.31) MUA attenuation due to SI inactivation was observed (figure 6 B and D). Furthermore, direct SI stimulation showed a burst of MUA activity (figure 6E, blue trace) with similar placement to CGIC-evoked MUA (figure 6A) and a slightly but significantly smaller latency (19.2 ±2.2ms; p=0.006) by ~6ms, which was completely eliminated by SI inactivation (figure 6E, red traces).

Discussion

It was found that CGIC is somatotopically organized (Rodgers et al., 2008). Since the Von Frey test is a good measure of allodynia in areas innervated by the sciatic nerve, it can be said that allodynia was successfully induced in animals using CCI ligations. Insular lesions were shown to attenuate allodynia in animals starting at about two weeks after CCI, but not before. This attenuation was found when CGIC was inactivated either before or after the allodynia-inducing condition was introduced. Spinally, a CGIC-evoked response was found in the spinal cord that was highly similar in timing and location to a late sciatic-evoked response that was

attenuated with CGIC or SI inactivation, unlike an earlier, shallower sciatic-evoked response not present on CGIC stimulation. Interestingly, a response similar in placement to the CGIC-evoked response but earlier in timing was also found.

A short discussion of insular lesions is required to address possible counterarguments against hypothesis to be put forth shortly. First, it should be noted that, according to Vogt, Hailer, Ghadban, Korf, and Dehghani (2008), if insular lesions that are complete (which those in this study were, judging from functional verification), the cortical damage should be finished (excitotoxic cell death or damage complete) within the waiting period that was given to animals in this study prior to CCI ligation (in the group of animals that received lesions before CCI). As such, during the initial development of allodynia in those animals, CGIC would already be fully lesioned. Before that, as was verified by extensive multi-threshold controls, CGIC lesions alone have no effect on observed acute pain development in animals. Also, it should again be mentioned that CGIC lesions were isolated, and extended neither to other somatosensory areas, nor into RAIC (Rodgers, et al., 2008), which is a previous focus of many pain experiments.

Two-Phase Model of Allodynia

Regardless of lesion status, all animals that received CCI ligations were found to develop allodynia maximum by 11 days post-CCI. This would indicate that CGIC played no role in allodynia onset in this time frame. However, starting at 14 days post-injury, a "recovery period" took place, where animals, regardless of having CGIC inactivated before or after CCI, had their allodynia attenuated over the course of two weeks back to baseline levels. These findings would suggest two distinct phases of allodynia – an initiation and a maintenance phase.

Two phases of allodynia time course have previously been proposed (Burgess et al., 2002). In the initiation part, sensitization of spinal pain mechanisms is argued to be a key player

(Saadé & Jabbur, 2008; Sandkühler, 2009), while the maintenance seems to be cortically modulated (Saadé & Jabbur, 2008; Campbell & Meyer, 2006). In accordance with these past data, the initiation phase we observed is likely not modulated by CGIC, since lesions had no effect on pain threshold depression. During the maintenance phase, CGIC inactivation was found to be sufficient in attenuation of allodynia. As such, it would make sense that, in accordance with past data, allodynia onset is likely spinally modulated (and/or, perhaps, as Burgess et al. (2002) suggest, also modulated by the rostral ventromedial medulla), and maintenance is CGIC-modulated. The "recovery phase" observation would therefore coincide with the two-week time period during which the spinal initiation influence is phased out for insular maintenance influence.

It may be argued that the initial phase of allodynia, rather than being attributed to the spinal cord, is caused by structural damage to the sciatic-innervated region of the rat hindleg during CCI ligation, and only the CGIC "maintenance" phase can truly be classified as chronic allodynia. One flaw with this argument is that, if anything, muscular damage should increase, not decrease threshold of withdrawal in general due to simple structural damage. Also, structural damage should not be observed to have a gradual, two-week onset as the initial phase was observed to have, but rather as an immediate drop in withdrawal threshold. Finally, CCI ligations and structural muscle damage are observed to be present far longer than the two-week initiation period (informal observation and unpublished data), which would make gradual pain recovery in lesion group animals unlikely to be correlated with simple tissue healing.

While previously, initiation and maintenance of allodynia were discussed as non-interconnected phenomena, this may not be the case. After carefully analyzing data this study

found on spinal MUA, and the timing and nature of events, a more interconnected and possibly causal (more data needed in this respect) mechanism of allodynia maintenance can be proposed.

Chronological Analysis of Cortically and Sciatic-Evoked Spinal MUA

It should be re-stated that the latency of CGIC-evoked spinal MUA is approximately 25ms, and is ~6ms more latent than SI-evoked MUA. Sciatic stimulation evokes similarly placed layer 4 MUA that at about ~43ms latency. Again, all of this latent MUA, except SI-evoked MUA, can be eliminated by inactivation of CGIC. At this point, it is important to mention that all of these latencies are far faster than the conduction time of C fiber from the sciatic to just the spinal cord alone, which takes over 100, and sometimes 200-300ms (You, Lei, & Arendt-Nielsen, 2009). As such, no MUA observed here has latencies large enough to warrant consideration of any C-fiber involvement whatsoever.

An analysis of the sciatic-evoked spinal layer 4 MUA, its time frame and likely causes of each specific MUA event is now in order. After an initial stimulus artifact, an almost immediate burst of activity is observed. Very likely, this is the sensory information from the sciatic stimulation arriving initially in the spinal cord. A second, ~43ms-latent MUA is also observed. Ruling out C-fiber signaling (due to previously mentioned conduction speed limitations), other ascending information from the sciatic nerve (which has already been accounted for), and intra-spinal processing (which would evoke continuous MUA after signal arrival that should not last as long as 43ms), the most logical cause for this latent MUA is descending modulation from the cortex *in response* to sciatic stimulation. Therefore, signals evoked by sciatic stimulation must be traveling to the spinal cord, cortex, and returned to the spinal cord – a spinal-cortex-spinal loop.

Considering how CGIC lesions attenuate the sciatic-evoked layer 4 ~43ms MUA, CGIC is a likely target for information traveling through the previously described spinocortical loop.

However, considering that because no descending corticospinal fibers originating in CGIC have ever been characterized, corticospinal information originating in CGIC must have an intervening brain region that must act as a relay between CGIC and the spinal cord. SI is an attractive candidate for this role. Indeed, when evoking layer 4 spinal MUA through cortical stimulation, SI evoked MUA are ~6ms faster than that evoked by CGIC, and SI inactivation attenuated the ability of CGIC to evoke MUA entirely. Therefore, 6ms can be considered as the time needed for processing and subsequent relay of corticospinal information from CGIC to SI. Overall, then, in a refinement of the spinal-cortex-spinal loop, information must be traveling to CGIC and be relayed to SI, which in turn sends signals back to the spinal cord.

When layer 4 spinal MUA was evoked through SI stimulation, a ~19ms latency was observed. Assuming this to be the conduction period needed for signals to travel "one way" between the cortex and the spinal cord (either from the spinal cord to CGIC, or from SI to the spinal cord) is not unreasonable. Besides that, since cortical electrophysiology employed in this study measures field potentials (postsynaptic dendrite potentials, which primarily show processing, not arrival) and not MUA (action potentials), the exact period needed for ascending information to reach CGIC cannot be reliably calculated based on present data. Going back to the spine-CGIC-SI-spine loop, two of these ~19ms conduction periods must be accounted for – one for ascending signals, and one for descending signals. Factoring in the previously described ~6ms delay for CGIC processing and relay of information to SI, the total time needed for information to travel from the spinal cord to CGIC, be relayed to SI, and be transmitted back to the spinal cord is ~19+6+19≈44ms. This value is strikingly similar to the observed latency of ~43ms sciatic-evoked late layer 4 MUA, giving even more evidence towards the spinal-CGIC-SI-spinal signaling loop.

Based on the previous analysis, a signaling pathway is proposed. Upon stimulation of regions innervated by the sciatic nerve, non-C fiber information is quickly conducted to the spinal cord. From there, these signals are transmitted to CGIC, where they are processed. CGIC then initiates descending spinal activity modulation by sending signals to SI, which relays them down to the spinal cord. This pathway is consistent with all temporal and cortical inactivation data in this study. This pathway also provides a way in which CGIC may be involved in pain perception; a notion that is demanded by the behavioral data in this study.

Proposed Mechanism of Maintenance of Allodynia

A mechanism is now proposed where two-way connectivity between CGIC and the spinal cord may serve to create a feedback loop that could maintain allodynia. If, during the initiation phase of allodynia, CGIC was caused to be continuously hyperactive, it could in turn maintain chronic spinal hyperactivation. High spinal activity could then send high amounts of ascending signals back to CGIC, creating positive feedback, which would maintain high spinal activity, and therefore high pain sensitivity (allodynia).

This mechanism fits into the two-phase model of allodynia. It also predicts that inactivation of CGIC at any point (not only initiation) would terminate this feedback and attenuate allodynia, which was indeed the case. Therefore, based on this mechanism, CGIC can be described as necessary and CGIC activity sufficient for the maintenance of allodynia, assuming otherwise normal cortical function (since, the proposed feedback model predicts that an inactive SI would make CGIC hyperactivation unable to induce allodynia alone).

Reviewing previous assertions, a spinal-CGIC-SI-spinal loop was proposed to play a key role in the maintenance, but not development, of allodynia. Permanent hyperactivation of CGIC during the development of allodynia was hypothesized to cause continuous hyperactivation of

the spinal cord (and so allodynia maintenance) through descending modulation. While this is the first study to propose such a mechanism, and therefore little data beside what is presented here can be used to support it, many future studies could be carried out to give further credibility to such a mechanism. Cytological data could be collected (and, indeed, was and is being collected in concurrence with this study by the Barth and collaborating laboratories) to show neuronal connectivity predicted by the mechanism proposed in this study. Also, sciatic-evoked MUA in CGIC could be observed to verify the ascending spinocortical conduction latency to be ~19ms as predicted. More broadly, MUA seen in this study could be repeated for allodynic animals, where the cortically and spinally evoked layer 4 spinal MUA is predicted to be significantly greater in magnitude or frequency. Another possibility of verifying the CGIC feedback model would be to chemically or electrically hyperactivate CGIC in living animals, which would be predicted to induce some form of allodynia, or at least prime animals for chronic pain – an effect that could be measured behaviorally. Even more broadly, other forms of chronic pain disorders (beside hindpaw allodynia) could be investigated in a similar fashion to this study to allow for generalization of the mechanism proposed here.

Given the model proposed by this study, new treatment of chronic pain could be possible. While CGIC lesion in humans is a highly extreme and non-recommended treatment, the fact that CGIC inactivation can attenuate allodynia even after initiation could make CGIC an attractive pharmaceutical target. Such pharmaceuticals could be used to effectively (since CGIC inactivation was shown to restore pain thresholds functionally to baseline) eliminate chronic pain symptoms within weeks of therapy initiation, and do so permanently through continuous administration, assuming no confounds such as tolerance – a common side effect for many analgesic drugs.

To summarize, data that suggest a mechanism for allodynia maintenance is presented. Future experiments can be conducted to give further support for this mechanism. However, even current data as is suggests an attractive target for treatment of chronic pain.

References

Alvarez, P., Dieb, W., Hafidi, A., Voisin, D. L., & Dallel, R. (2009). Insular cortex representation of dynamic mechanical allodynia in trigeminal neuropathic rats. *Neurobiology of Disease, 33*, 89-95.

Becerra, L., Morris, S., Bazes, S., Gostic, R., Sherman, S., Gostic, J., … Borsook, D. (2006). Trigeminal neuropathic pain alters responses in CNS circuits to mechanical (brush) and thermal (cold and heat) stimuli. *Journal of Neuroscience, 26*, 10646-10657.

Benison, A. M., Rector, D. M. & Barth, D. S. (2007). Hemispheric mapping of secondary somatosensory cortex in the rat. *Journal of Neurophysiology,* 97, 200-207.

Brooks, J. C. W., Zambreanu, L., Godinez, A., Craig, A. D., Tracey, I. (2005). Somatotopic organization of the human insula to painful heat studied with high-resolution functional imaging. *NeuroImage, 27*(1), 201-209.

Burgess, S. E., Gardell, L. R., Ossipov, M. H., Malan, T. P. Jr., Vanderah, T. W., Lai, J., & Porreca, F. (2002). Time-dependent descending facilitation from the rostral ventromedial medulla maintains, but does not initiate, neuropathic pain. *Journal of Neuroscience, 22*, 5129-5136.

Campbell, J. N., & Meyer, R. A. (2006). Mechanisms of neuropathic pain. *Neuron, 52*(1), 77-92.

Chaplan, S. R., Bach, F. W., Pogrel, J. W., Chung, J. M., & Yaksh, T. L. (1994). Quantitative assessment of tactile allodynia in the rat paw. *Journal of Neuroscience Methods, 53*, 55-63.

Coffeen, U., Ortega-Legaspi, M. J., López-Muñoz, F. J., Simón-Arceo, K., Jaimes, O., & Pellicer, F. (2011). Insular cortex lesion diminishes neuropathic and inflammatory pain-like behaviours. *European Journal of Pain,* 15, 132-138.

Davis, K. D., Taub, E., Duffner, F., Lozano, A. M., Tasker, R. R., Houle, S., & Dostrovsky, J. O. (2000). Activation of the anterior cingulate cortex by thalamic stimulation in patients with chronic pain: a positron emission tomography study. *Neurosurgical Focus, 92*(1), 64-69.

Derbyshire, S. W. G., Jones, A. K. P., Gyulai, F., Clarck, S., Townsend, D., & Firestone, L.L. (1997). Pain processing during three levels of noxious stimulation produces differential patterns of central activity. *Pain, 73*, 431-445.

Elliott, A. M., Smith, B. H., Penny, K. I., Smith, W. C., & Chambers, W. A. (1999). The epidemiology of chronic pain in the community. *The Lancet*, *354,* 1248-1252.

Jasmin, L., Rabkin, S. D., Granato, A., Boudah, A., & Ohara, P. T. (2003). Analgesia and hyperalgesia from GABA-mediated modulation of the cerebral cortex. *Nature, 424*, 316-320.

Lamour, Y., Willer, J. C., & Guilbaud, G. (1982). Neuronal responses to noxious stimulation in rat somatosensory cortex. *Neuroscience Letters, 29*, 35-40.

Li, X. Y., Ko, H. G., Chen, T., Descalzi, G., Koga, K., Wang, H., … Zhuo, M. (2010). Alleviating neuropathic pain hypersensitivity by inhibiting PKMzeta in the anterior cingulate cortex. *Science, 330*, 1400-1404.

Lorenz, J., Minoshima, S., & Casey, K. L. (2003). Keeping pain out of mind: the role of the dorsolateral prefrontal cortex in pain modulation. *Brain, 126*, 1079-1091.

Luis-Delgado, O. E., Barrot, M., Rodeau, J. L., Schott, G., Benbouzid, M., Poisbeau, P., … Lasbennes, F. (2006). Calibrated forceps: a sensitive and reliable tool for pain and analgesia studies. *The Journal of Pain, 7*, 32-39.

Melzack R., & Casey K. L. (1968). Sensory, motivational and central control determinants of pain. In D. R. Kenshalo (Ed.), *The skin senses* (pp. 423-439). Springfield, IL: Charles C. Thomas.

Milligan, E. D., Soderquist, R. G., Malone, S. M., Mahoney, J. H., Hughes, T. S., Langer, S. J., … Mahoney, M. J. (2006a). Intrathecal polymer-based interleukin-10 gene delivery for neuropathic pain. *Neuron Glia Biology, 2*, 293-308.

Milligan, E. D., Sloane, E. M., Langer, S. J., Hughes, T. S., Jekich, B. M., Frank, M. G., … Watkins, L. R. (2006b). Repeated intrathecal injections of plasmid DNA encoding interleukin-10 produce prolonged reversal of neuropathic pain. *Pain, 126*, 294-308.

Ohara, P. T., Vit, J. P., & Jasmin, L. (2005). Cortical modulation of pain. *Cellular and Molecular Life Sciences, 62*, 44-52.

Ostrowsky, K., Magnin, M., Ryvlin, P., Isnard, J., Guenot, M., Mauguie`re, F. (2002). Representation of pain and somatic sensation in the human insula: a study of responses to direct electrical cortical stimulation. *Cerebral Cortex, 12*, 376-385.

Paulus, M. P., & Stein, M. B. (2006). An insular view of anxiety. *Biological Psychiatry, 60*(4), 383-387.

Peyron, R., García-Larrea, L., Grégoire, M. C., Convers, P., Lavenne, F., Veyre, L., … Laurent, B. (1998). Allodynia after lateral-medullary (Wallenberg) infarct. A Positron Emission Tomography (PET) study. *Brain, 121*, 345-356.

Peyron, R., Laurent, B., & Garcia-Larrea, L. (2000). Functional imaging of brain responses to pain. A review and meta-analysis. *Clinical Neurophysiology, 30*, 263–288.

Reynolds, S. M., & Zahm, D. S. (2005). Specificity in the projections of prefrontal and insular cortex to ventral striatopallidum and the extended amygdala. *Journal of Neuroscience,* 25, 11757-11767.

Rodgers, K. M., Benison, A. M., Klein, A. & Barth, D. S. (2008). Auditory, somatosensory, and multisensory insular cortex of the rat. *Cerebral Cortex,* 18, 2941-2951.

Saadé, N. E., & Jabbur, S. J. (2008). Nociceptive behavior in animal models for peripheral neuropathy: spinal and supraspinal mechanisms. *Progress in Neurobiology, 86*, 22-47.

Sandkühler, J. (2009). Models and mechanisms of hyperalgesia and allodynia. *Physiological Reviews, 89*, 707-758.

Sloane, E., Langer, S., Jekich, B., Mahoney, J., Hughes, T., Frank, M., … Milligan, E. (2009). Immunological priming potentiates non-viral anti-inflammatory gene therapy treatment of neuropathic pain. *Gene Therapy, 16*, 1210-1222.

Treede, R. D., Kenshalo, D. R., Gracely R. H., & Jones, A. K. (1999). The cortical representation of pain. *Pain, 79*, 105-111.

Vogt, C., Hailer, N. P., Ghadban, C., Korf, H. W., & Dehghani, F. (2008). Successful inhibition of excitotoxic neuronal damage and microglial activation after delayed application of interleukin-1 receptor antagonist. *Journal of Neuroscience Research, 86*, 3314-3321.

You, H. J., Lei, J., & Arendt-Nielsen, L. (2009). Selective inhibitory effects of pregabalin on peripheral C but not A-delta fibers mediated nociception in intact and spinalized rats. *Neuroscience, 164*, 1845-1853.

Figures

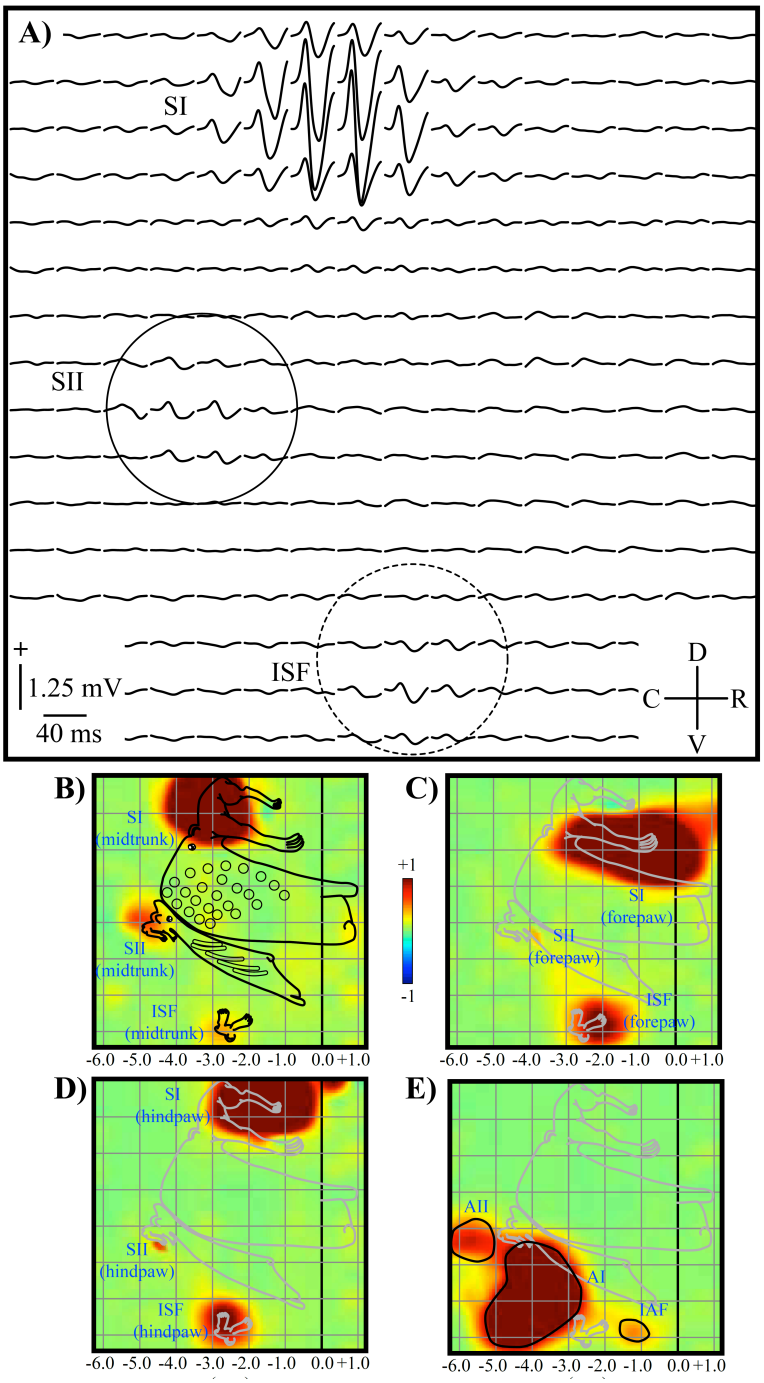

Figure 1. Functional EP mapping of CGIC and other somatosensory regions. A) Averaged somatosensory right hemisphere EPs plotted as voltage over time for each electrode in the 16x16 electrode array, evoked by mid-trunk stimulation, with SI, SII and CGIC located as labeled. B-E) RMS map (of raw responses seen in A) of right hemisphere mid-trunk (B), forepaw (C), hindpaw (D) and auditory (E) EPs, with ratunculus superimposed. X coordinates refer to distance from bregma (located over 0.0 vertical bold line).

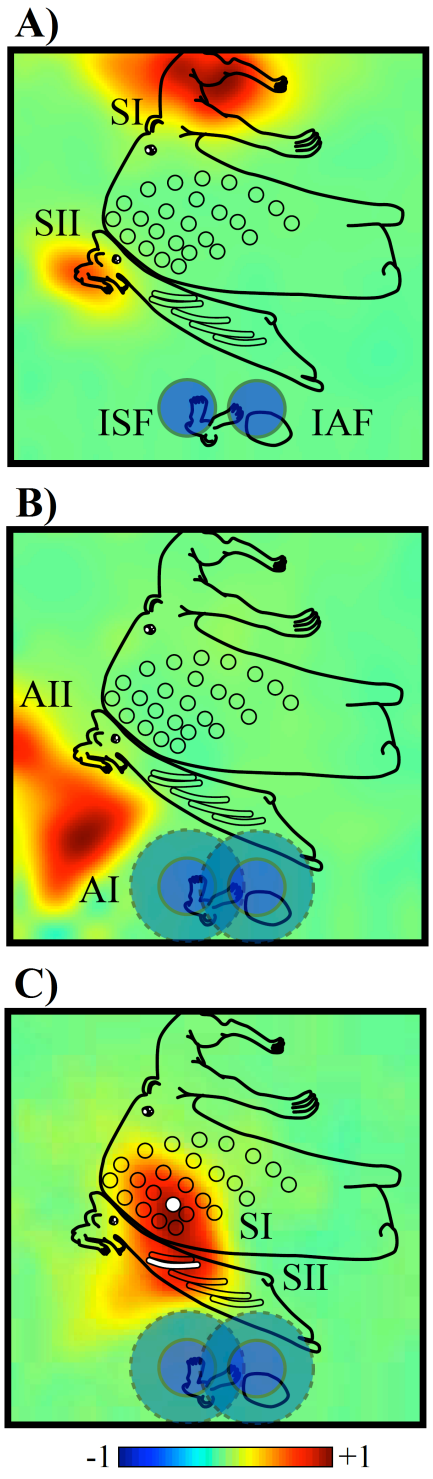

Figure 2. Functional insular lesion verification. RMS maps show EPs from stimulation of the mid-trunk (somatosensory area; A), auditory stimulation (B) or stimulation of the B2 whisker (C) with functionally established areas as labeled, and ratunculus superimposed. Large blue circles indicate CGIC lesion sites, and where otherwise present responses are absent.

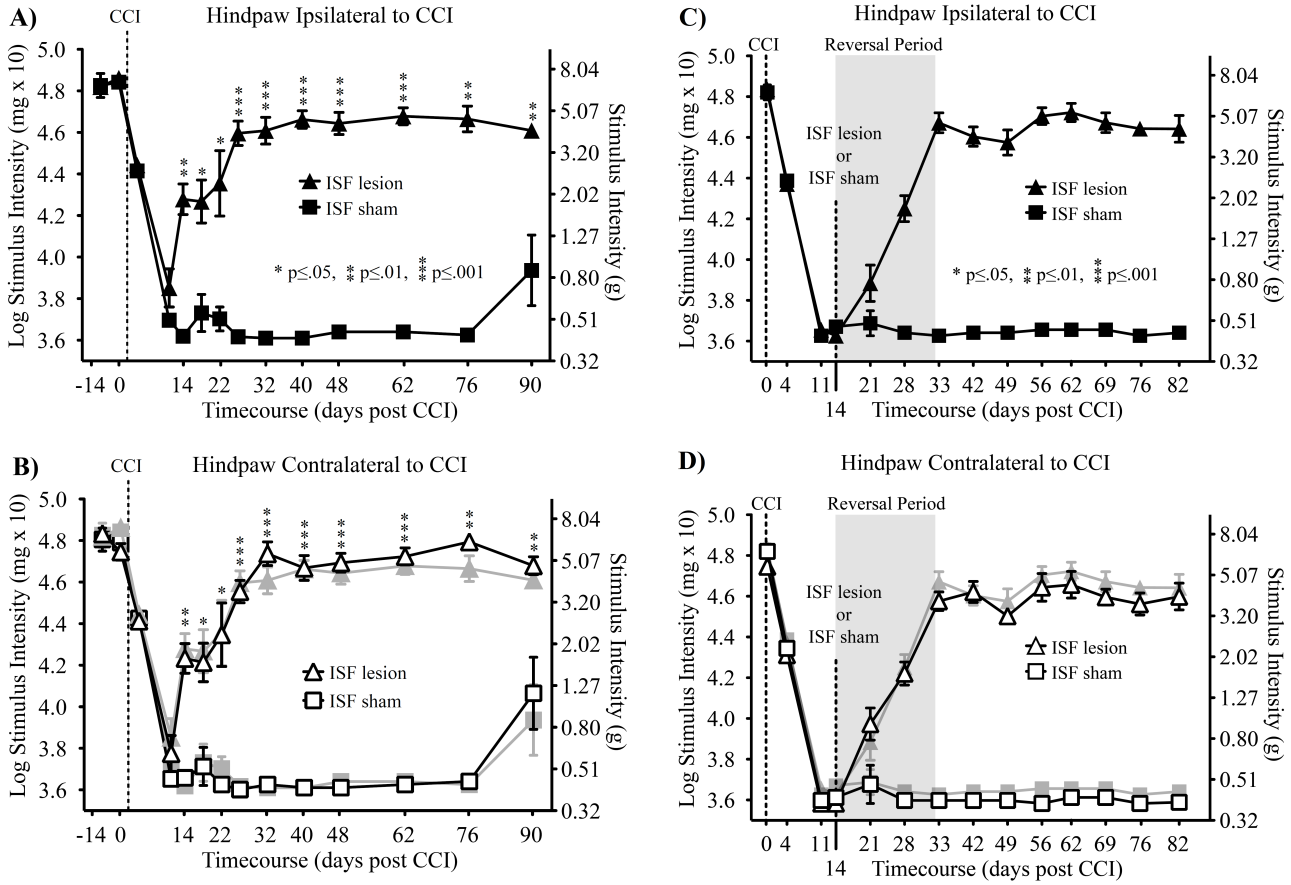

Figure 3. CGIC lesions both before and shortly after CCI ligation prevent long-term maintenance of allodynic responses. Allodynia was quantified by the von Frey test, with stimulus intensity withdrawal threshold indicated by the Y axes. For all subfigures, the first time point represents baseline measurements and the dashed line – point of CCI ligation (0 point on the X axes). Experimental groups in terms of ISF lesion status are as labeled; all animals received CCI ligations. When CCI ligations are administered 14 days post-CGIC lesion (A, B), experimental group threshold depression reversal can be seen both ipsilaterally to CCI (A), and contralaterally (mirror pain, B, where ipsilateral responses are shown greyed out in the background) after 14 days. When lesions are administered after CCI ligation (C, D), during the reversal period (grey bar) stimulus response thresholds rebound in experimental animals both ipsilaterally to CCI (C) and contralaterally (mirror pain, D).

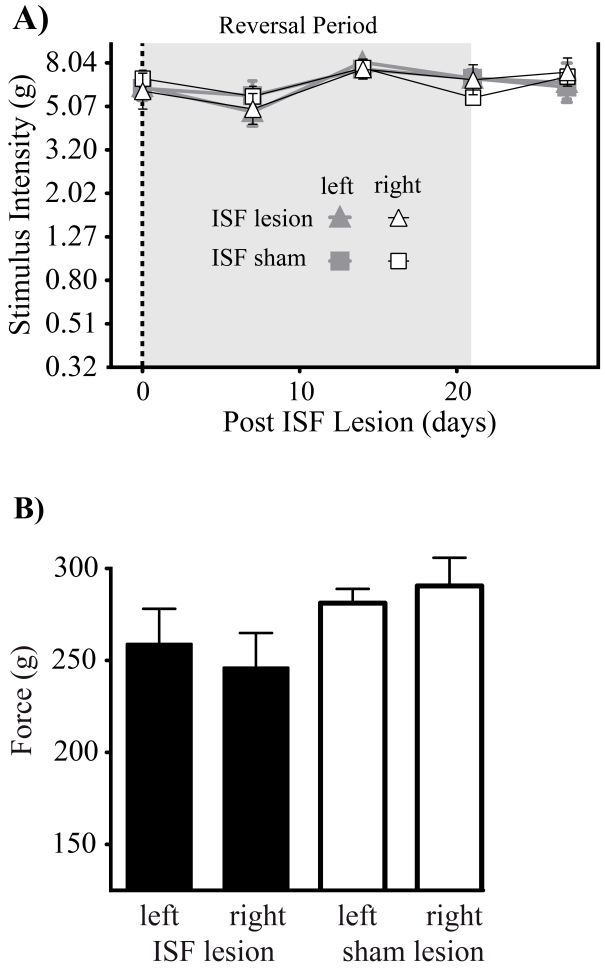

Figure 4. Insular lesion behavioral control. A) Low threshold pain control. In insularly lesioned (days post lesion on X axis, with baseline taken before lesion administration on day 0) animals that never received CCI ligations, von Frey testing (stimulus intensity on Y axis) was used to quantify low-threshold pain responses in left and right hindpaws (as labeled). The reversal period as seen in figure 3 is highlighted. All experimental groups as labeled, with no significant difference in responses over time found. B) High-threshold pain control. Force required from calibrated toe pinch to elicit withdrawal labeled on Y axis. Experimental groups as labeled, with no significant withdrawal threshold difference found.

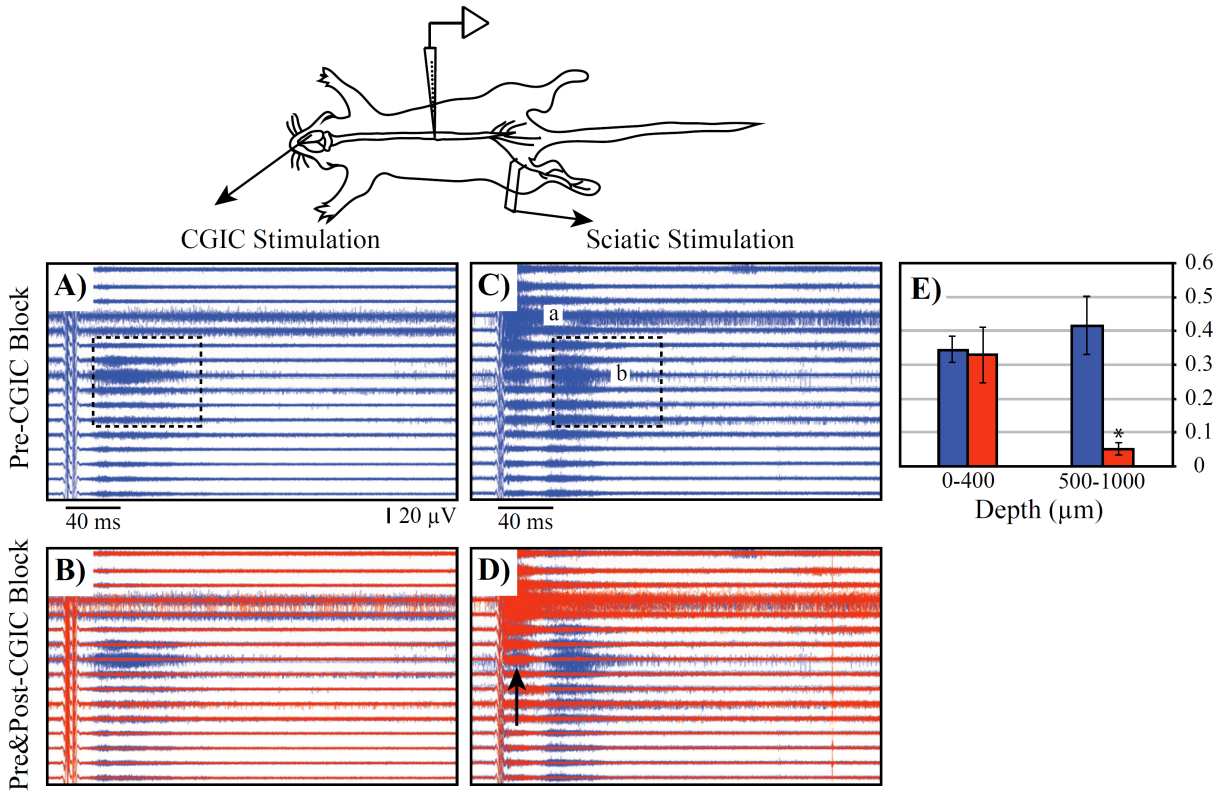

Figure 5. Effects of CGIC inactivation on spinal MUA. The schematic on top depicts areas of stimulation (with labels over corresponding MUA recording columns), and the 16-channel laminar recording electrode (white arrow on top). Note that subfigures A-D depict 64 superimposed trials of a single animal, with the X axes corresponding to time and lower traces corresponding to deeper electrodes in the spinal cord. A) depicts observed baseline MUA in response to CGIC stimulation. The dashed box corresponds to MUA that is eliminated in the red traces of B, which show CGIC-evoked MUA after CGIC inactivation, compared to control animals in the background blue traces. C) shows MUA evoked by sciatic stimulation, where early, shallow MUA is labeled by a, and deep, later MUA by b and a dashed box. D) shows sciatic-evoked MUA after CGIC inactivation (red) compared to control (blue), where a is seen to persist, and b is attenuated. The black arrow shows visible yet non-significant attenuation in MUA of same depth but earlier to b. E) depicts maximum MUA magnitude (normalized to the maximum MUA of all electrodes in each particular animal, and so range 0 – 1.0) and the significance of attenuation of MUA “a” (0-400) and “b” (500-1000µm depth) seen in D (blue bars show average MUA magnitude in control animals, while red bars show average MUA in animals where CGIC was inactivated).

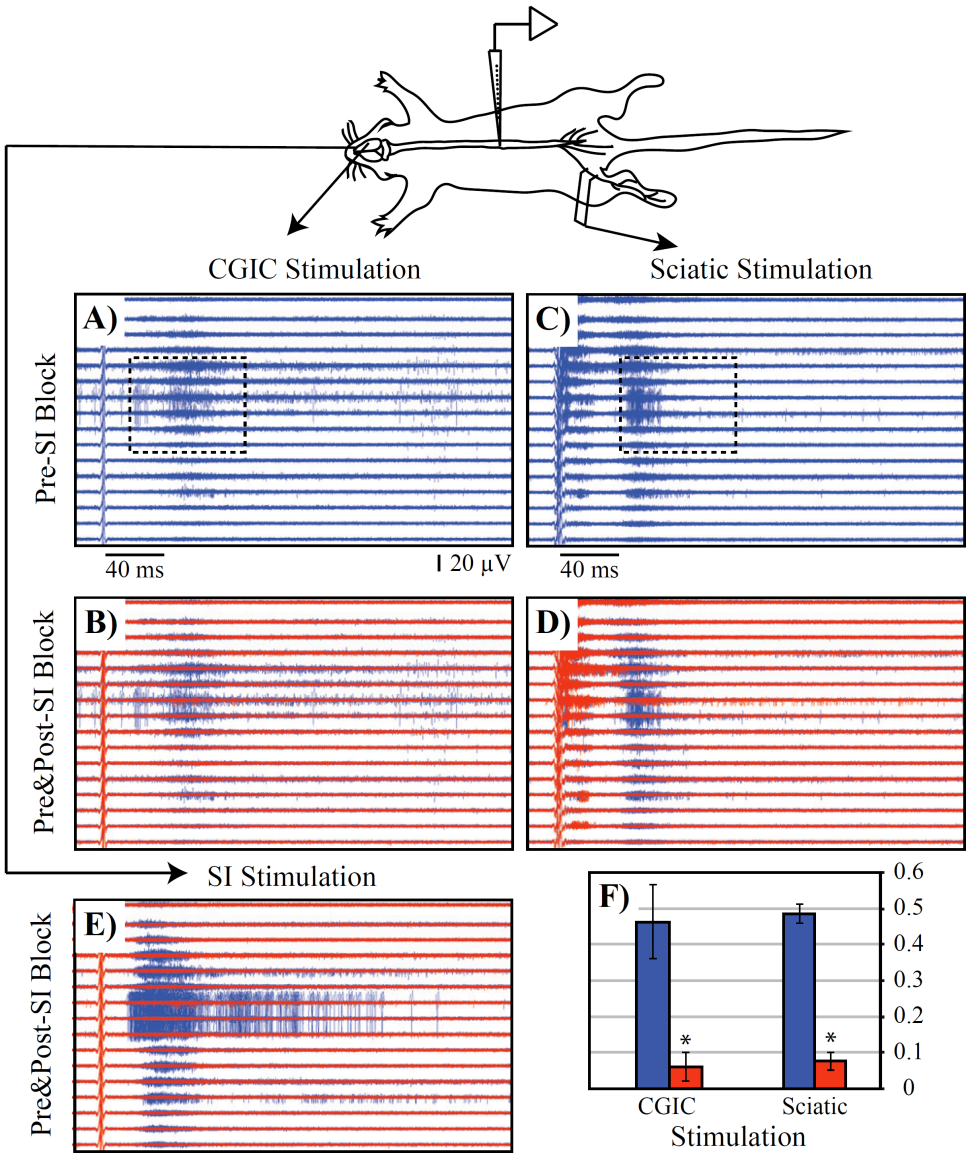

Figure 6. Effects of SI inactivation on spinal MUA. The rat schematic on top serves the same function as in figure 5. Note here also that subfigures A-E depict 64 superimposed trials of a single animal, with the X axes corresponding to time and lower traces corresponding to deeper electrodes in the spinal cord. A) shows CGIC-evoked MUA, where an MUA burst can be seen in the dashed box that is attenuated after inactivation of SI, as seen in the red traces in B when compared to the control blue traces. C) shows sciatic-evoked MUA, where a boxed MUA burst is also observed, and is attenuated by SI inactivation as seen in red traces of D as compared to control blue traces. E) shows MUA evoked by SI stimulation, before (blue traces) and after SI inactivation (red traces, where all SI responses are eliminated entirely). F) quantifies and establishes significance of attenuation of boxed MUA from A ("CGIC" bars) and C ("Sciatic" bars) in response to SI inactivation (control group blue bars versus experimental/SI inactivated group red bars), where MUA magnitude (Y axis) was analyzed in a similar manner to figure 5E.